

Morphology of Ionomers

Curtis L. Marx,^{1a} Daniel F. Caulfield,^{1b} and Stuart L. Cooper*

Chemical Engineering Department, University of Wisconsin, Madison, Wisconsin 53706.
Received August 24, 1972

ABSTRACT: A new "aggregate" model for ionomers is presented. The model is similar to the "homogeneous" model in that the acid aggregate distribution is assumed to be homogeneous and similar to the "cluster" model in that acid groups are assumed to aggregate. The aggregate model, however, differs from the other models in that the degree of aggregation is low and affected by carboxyl group concentration and the presence of polar diluent. The aggregates are much smaller than the clusters previously theorized. New data obtained by wide and small-angle X-ray scattering and differential scanning calorimetry are presented. These techniques are used to study the X-ray peaks attributed to ionic clusters. Changes in the X-ray scattering behavior of ionomers with composition are interpreted in terms of an increase in the number of carboxyl groups per scattering site. The aggregation increases from dimers to trimers to tetramers up to septimers as the acid content in the copolymer increases. Plasticization with water is shown to further increase the extent of carboxyl group aggregation.

The word "ionomer" was coined to describe polymers with the capability of forming intermolecular ionic bonds. It is a generic term used to include polymers containing pendant carboxylic salt groups on a polyolefin backbone.^{2a} These polymers (P) are generally prepared by copolymerizing an olefin, such as ethylene (E), butadiene (B), or styrene (S) with a carboxylic acid, such as acrylic acid (AA) or methacrylic acid (MAA). The copolymers thus formed are then ionized to form ionomers.

Two morphological models have been proposed to rationalize the properties of polyethylene ionomers. Evidence has been presented to support and refute each model.^{2b} The two models are the "homogeneous" model in which the carboxylic salt groups are assumed to be randomly distributed in the amorphous phase of the polymer, and the "cluster" model in which salt groups are thought to aggregate in clusters about 100 Å in diameter.

Homogeneous Model. The homogeneous model consists of a crystalline phase and an amorphous phase. The acid groups and their salts are assumed to be randomly distributed as dimers in the amorphous phase. Evidence supporting this model has been obtained by nmr, X-ray analysis, and glass transition shift with composition.

Nuclear magnetic resonance data obtained by Ostocka and Davis³ indicates that the γ and β transition temperatures for lithium in an ethylene-lithium acrylate copolymer very closely match the transition temperatures of protons in this ionomer. From this it was inferred that the lithium nuclei are randomly distributed in the matrix material and not isolated in large ionic clusters.

Roe⁴ did a Fourier transform analysis of X-ray scattering data for an ethylene-acrylic acid (E-AA) copolymer and its cesium salt. He subtracted the distribution function for the copolymer from that of the salt to obtain the interaction spacings between cesium and other atoms. This difference function indicated a minimum spacing of about 2.4 Å and a Cs-O spacing of about 3.1 Å. Additional spacings of 4.5 and 5.0 Å were shown to be about the same magnitude observed for Cs-Cs spacings in other materials. Spacings between 6 and 16 Å were absent. From this evidence and other arguments he concluded that there was a lack of evidence for ionic clusters 15 Å in size

or smaller, but that there was evidence for dimer formation.

Ostocka and Kwei⁵ found that for sodium and magnesium salts of E-AA copolymers the low temperature amorphous β transition increases according to copolymerization theories, indicating that the salt groups are well distributed in the amorphous phase.

Other evidence has been presented which was interpreted as being inconsistent with the homogeneous model. This led to formulation of the "cluster" model.

Cluster Model. The cluster model consists of a crystalline and an amorphous phase with ionic clusters about 100 Å in diameter embedded in the amorphous phase. Evidence interpreted as supporting this model has been obtained by wide-angle X-ray scattering, electron microscopy, low-angle X-ray scattering, and mechanical relaxation studies.

The cluster model was proposed by Longworth and Vaughan^{6,7} to account for results obtained by wide-angle X-ray scattering measurements on polyethylene ionomers.⁸⁻¹⁰ A peak corresponding to a Bragg spacing of about 20 Å appears in the X-ray scattering of ionomers that is not present in the scattering from the unionized copolymers. Since the peak was observed for all cations studied including lithium, it was concluded that the peak does not result from the electron-density difference between the cation and the polymer, but from an electron density difference resulting from a change of morphology upon ionization. They reasoned that "for a peak to be observed at all, there is a rule of thumb . . . that at least five repeat units are required. This would put a lower limit of 100 Å on the linear dimensions of ionic phase domains."⁸ The Bragg spacing was observed to decrease with increasing acid content and increase with increasing ionization. No explanation has previously been offered for this behavior. The peak was observed to persist to at least 300°, although these materials melt at about 100°.

Water was reported to have the following effect on the ionomer X-ray peak. "Low levels of humidity will enhance the intensity of the peak, but saturating the sample with water will virtually destroy it."⁸ It was concluded that the

(1) (a) Present address: E. I. du Pont de Nemours & Company, Waynesboro, Virginia 22980; (b) U.S.D.A. Forest Products Laboratory, Madison, Wis.

(2) (a) "Modern Plastics Encyclopedia," McGraw-Hill, New York, N. Y., 1968, p 208; (b) E. P. Ostocka, *J. Macromol. Sci., Part C*, **5**, 275 (1971).

(3) E. P. Ostocka and D. D. Davis, *Macromolecules*, **2**, 437 (1969).

(4) R. J. Roe, *Polym. Prepr., Amer. Chem. Soc., Div. Polym. Chem.*, **12**, 730 (1971).

(5) E. P. Ostocka and T. K. Kwei, *Macromolecules*, **1**, 401 (1968).

(6) R. Longworth and D. J. Vaughan, *Nature (London)*, **218**, 85 (1968).

(7) R. Longworth and D. J. Vaughan, *Polym. Prepr., Amer. Chem. Soc., Div. Polym. Chem.*, **9**, 525 (1968).

(8) F. C. Wilson, R. Longworth, and D. J. Vaughan, *Polym. Prepr., Amer. Chem. Soc., Div. Polym. Chem.*, **9**, 505 (1968).

(9) R. W. Rees and D. J. Vaughan, *Polym. Prepr., Amer. Chem. Soc., Div. Polym. Chem.*, **6**, 287 (1965).

(10) E. P. Ostocka, *Org. Coat. Plast. Chem.*, **32**, 45 (1972).

effect of water is to solvate the ionic regions and destroy order within them.

Electron microscopic investigations have been interpreted as possible evidence for the cluster model. Davis, Longworth, and Vaughan¹¹ and Rees and Vaughan⁹ reported structures in polyethylene ionomers thought to be ionic clusters. Recent work by Phillips¹² suggests clusters in amorphous poly(ethylenephosphonic acid) ionomers. Marx, Koutsky, and Cooper¹³ reporting on butadiene-methacrylic acid copolymers found small structures by electron microscopy. Additional questions regarding focusing¹⁴ and staining artifacts in high-resolution electron microscopy must be resolved before these results can be incorporated into a morphological model.

Small-angle X-ray scattering data has been reported which was interpreted in terms of the cluster model. Delf and MacKnight¹⁵ reported that a small-angle X-ray scattering peak appears in a cesium or sodium ionized ethylene-methacrylic acid copolymer which is not present in a lithium ionomer or in the unionized copolymer. The peak corresponded to a Bragg spacing of about 83 Å. They reported that the peak was not affected by annealing. Eisenberg and Navratil^{16,17} observed a small angle peak in cesium salts of styrene-methacrylic acid copolymers containing more than 6 mol % MAA. The peak corresponded to a Bragg spacing of 60–80 Å. The presence of a 20- and an 80-Å peak has been interpreted¹⁸ in terms of intradomain and interdomain spacings of the ionic clusters.

Dynamic mechanical, dielectric, and proton magnetic relaxation studies of E-MAA and E-AA copolymers and their salts have revealed changes in relaxation mechanisms near room temperature resulting from copolymerization and ionization. Although Otocka and Kwei⁵ interpreted dynamic relaxation data to be in support of the homogeneous model, Longworth and Vaughan^{6,7} and MacKnight *et al.*^{19,20} interpreted it as being consistent with the cluster model. Likewise, stress relaxation data^{21–25} has in some cases been interpreted as being consistent with the cluster model.

X-Ray orientation,²⁶ birefringence,²⁷ and an infrared orientation study²⁸ have indicated that a transition occurs in E-MAA ionomers that is not present in the unionized copolymer. This was interpreted as being caused by a softening transition in ionic domains.

Infrared studies of ionomers have indicated that most of the acid groups are hydrogen bonded, indicating associa-

Table I
Ionomer Characterization

Carboxyl Content (equiv/100 g)	Co-polymer	Metal Ion	Ion Content (equiv/100 g)	Wt % MAA	% Ionized
0.13	E ^a	None	0	11	0
0.12	E	Na	0.06	10	50
0.12	E	Na	0.08	10	75
0.14	E	Zn	0.03	12	22
0.14	E	Zn	0.08	12	57
0.17	E	Na	0.05	15	29
0.17	E	Zn	0.10	15	59
0.19	E	Na	0.07	16	37
0.082	B ^b	None	0	7	0
0.125	B	None	0	10.5	0
0.209	B	None	0	18	0

^a Poly(ethylene-methacrylic acid). ^b Poly(butadiene-methacrylic acid).

tion with one or more other acid groups.^{29–37} The possibility of acid group association has also been suggested by the similarity of the effect of monovalent and divalent ions on the viscosity^{37–39} and bulk properties^{9,30,40,41} of ionomers. In addition, many properties of ionomers are approximately constant for ionization levels greater than one-third, indicating trimer association.^{9,38} Read, Carter, Connor, and MacKnight²⁰ analyzed dielectric data for the β relaxation assuming a monomer-dimer equilibrium. The analysis predicted too small a magnitude for the transition. They suggested that the presence of trimers or tetramers was a possible explanation for the discrepancy.

In summary, evidence has been cited which supports and contradicts both the "cluster" and "homogeneous" models with and without modification to include the concept of multiplets. A new perspective was required to reconcile the discrepancies.

Experimental Section

Poly(ethylene-methacrylic acid) ionomers were obtained from the Du Pont Co. Poly(butadiene-methacrylic acid) copolymers were obtained through the courtesy of Dr. E. A. Collins of the B. F. Goodrich Chemical Co. The butadiene copolymers contained Santovar A-CaO-1 anti-oxidants (0.5:2.5). Characterization data for samples received is presented in Table I.

One per cent butadiene-MAA polymer solutions in benzene-dioxane (80:20) or toluene-H₄furan (60:40) were prepared. These were titrated with 0.1 N sodium methoxide in benzene-methanol (80:20) under nitrogen. The sodium methoxide solution was standardized with benzoic acid in benzene-dioxane (80:20) using Thymol Blue as indicator. The copolymer acid contents were determined by titration under nitrogen using Thymol Blue

- (11) H. A. Davis, R. Longworth, and D. J. Vaughan, *Polym. Prepr., Amer. Chem. Soc., Div. Polym. Chem.*, **9**, 515 (1968).
- (12) P. J. Phillips, *J. Polym. Sci., Part B*, **10**, 443 (1972).
- (13) C. L. Marx, J. A. Koutsky, and S. L. Cooper, *J. Polym. Sci., Part B*, **9**, 167 (1971).
- (14) C. L. Marx, Ph.D. Thesis, Univ. of Wisconsin (1972).
- (15) B. W. Delf and W. J. MacKnight, *Macromolecules*, **2**, 309 (1969).
- (16) A. Eisenberg and M. Navratil, *J. Polym. Sci., Part B*, **10**, 537 (1972).
- (17) A. Eisenberg and M. Navratil, *Helsinki IUPAC Prepr., Bulk Prop.*, **69** (1972).
- (18) A. Eisenberg, *Macromolecules*, **3**, 147 (1970).
- (19) W. J. MacKnight, T. Kajiyama, and L. W. McKenna, *Polym. Eng. Sci.*, **8**, 267 (1967).
- (20) B. E. Read, E. A. Carter, T. M. Connor, and W. J. MacKnight, *Brit. Polym. J.*, **1**, 123 (1969).
- (21) E. P. Otocka and F. R. Eirich, *J. Polym. Sci., Part A-2*, **6**, 913 (1968).
- (22) E. P. Otocka and F. R. Eirich, *J. Polym. Sci., Part A-2*, **6**, 921 (1968).
- (23) A. V. Tobolsky, P. F. Lyons, and N. Hata, *Macromolecules*, **1**, 515 (1968).
- (24) A. V. Tobolsky and M. C. Shen, *J. Phys. Chem.*, **67**, 1886 (1963).
- (25) T. C. Ward and A. V. Tobolsky, *J. Appl. Polym. Sci.*, **11**, 2403 (1967).
- (26) T. Kajiyama, T. Oda, R. S. Stein, and W. J. MacKnight, *Macromolecules*, **4**, 198 (1971).
- (27) T. Kajiyama, R. S. Stein, and W. J. MacKnight, *J. Appl. Phys.*, **41**, 4361 (1970).
- (28) Y. Uemura, R. S. Stein, and W. J. MacKnight, to be published.

- (29) W. Cooper, *J. Polym. Sci.*, **28**, 195 (1958).
- (30) W. E. Fitzgerald and L. E. Nielsen, *Proc. Roy. Soc., Ser. A*, **282**, 137 (1964).
- (31) R. Longworth and H. Morawetz, *J. Polym. Sci.*, **29**, 307 (1958).
- (32) W. J. MacKnight, L. W. McKenna, B. E. Read, and R. S. Stein, *Polym. Prepr., Amer. Chem. Soc., Div. Polym. Chem.*, **8**, 1130 (1967); *J. Phys. Chem.*, **72**, 1122 (1968).
- (33) E. P. Otocka and F. R. Eirich, *J. Polym. Sci., Part A-2*, **6**, 895 (1968).
- (34) E. P. Otocka and T. K. Kwei, *Macromolecules*, **1**, 244 (1968); *Polym. Prepr., Amer. Chem. Soc., Div. Polym. Chem.*, **9**, 1 (1968).
- (35) E. P. Otocka and T. K. Kwei, *Soc. Plast. Eng., Antec.*, **15**, 23 (1969).
- (36) A. T. Tsatsas and W. M. Risen, Jr., *Chem. Phys. Lett.*, **7**, 354 (1970).
- (37) E. P. Otocka, M. Y. Hellman, and L. L. Blyler, *J. Appl. Phys.*, **40**, 4221 (1969).
- (38) S. Bonotto and E. F. Bonner, *Macromolecules*, **1**, 510 (1968).
- (39) N. Z. Erdi and H. Morawetz, *J. Colloid Sci.*, **19**, 708 (1964).
- (40) K. Sakamoto, W. J. MacKnight, and R. S. Porter, *J. Polym. Sci., Part A-2*, **8**, 277 (1970).
- (41) W. J. MacKnight, T. Kajiyama, and L. W. McKenna, *Polym. Prepr., Amer. Chem. Soc., Div. Polym. Chem.*, **9**, 534 (1968).

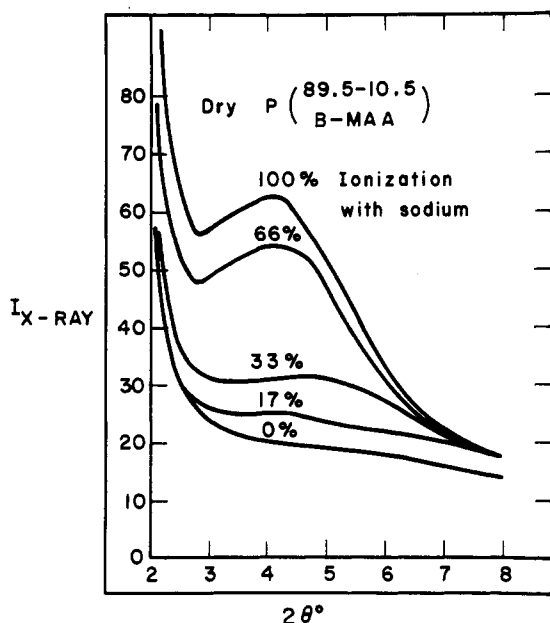


Figure 1. Effect of ionization on the ionomer X-ray peak of a dry B-MAA copolymer containing 10.5 wt % MAA.

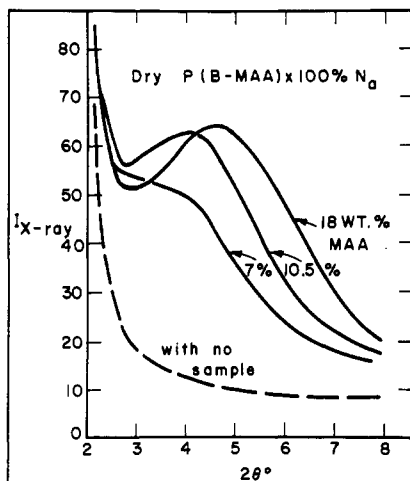


Figure 2. Effect of acid content on the ionomer X-ray peak of dry B-MAA copolymers completely ionized with sodium.

as indicator. Compositions determined were in agreement with values reported by B. F. Goodrich which appear in Table I. Samples of a desired degree of ionization were prepared by adding the amount of sodium methoxide solution calculated to be required. Ionization with cesium was accomplished by titrating the polymer solution with an 0.2 N solution of cesium hydroxide in methanol. Solutions were cast in Teflon pans to allow solvent evaporation.

Prior to molding samples were dried overnight in a vacuum oven. Polybutadiene and polyethylene ionomers were dried at about 80 and 110°, respectively, and molded at 150 and 170°, respectively, at about 8000 psi. All samples were stored in dessicators following molding.

Poly(methacrylic acid) was obtained from Polysciences, Inc. It was dissolved in water and titrated with an aqueous sodium hydroxide solution. The ionized polymer was cast, dried in a vacuum oven overnight at 110°, and then molded at 225° and 14,000 psi. The unionized polymer was dried then molded at 205° and 14,000 psi.

Wide-angle X-ray scattering was conducted using a Picker Model 2861 diffractometer with samples mounted for symmetrical transmission. Copper radiation was used in both wide- and low-angle scattering in conjunction with a nickel filter. Slits of 1° were employed for wide-angle scattering and two pin holes of 0.3- and 0.5-mm diameter at a separation of 20 cm. were employed for low-angle scattering. A counter was used to scan the wide-angle scattering. Low-angle scattering was recorded on photographic film using a Rigaku Denki Model scattering goniometer. The film

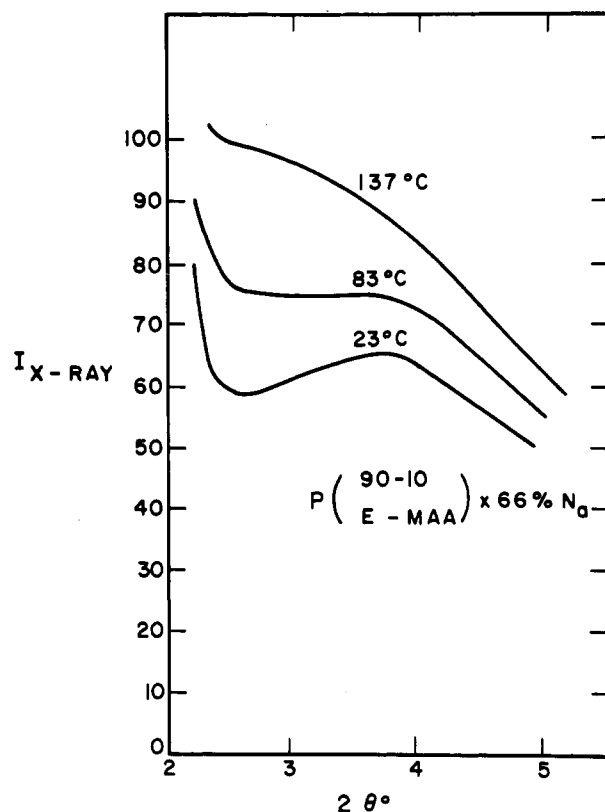


Figure 3. Effect of temperature on the ionomer X-ray peak of a 90-10 wt % E-MAA copolymer ionized 66% with sodium.

was later scanned with a Joyce-Lobel double-beam microdensitometer. Film exposure times of 8 and 24 hr were employed.

The thickness of polyethylene, ethylene copolymer and ionomer, and butadiene copolymer and ionomer samples was standardized at 1.9 mm to allow a direct comparison of X-ray scattering between samples. Ionized poly(methacrylic acid) samples and samples ionized with cesium were thinner. The optimum thickness for these samples was calculated, then confirmed experimentally.

Partially ionized acid samples were contained in polyethylene bags. The high-temperature experiments used a specially constructed sample holder with Mylar windows. Dry samples used for low-angle X-ray scattering were sealed in 0.00025-in. thick Mylar bags containing a desiccant. Background scattering from the polyethylene and Mylar bags was determined and found to be negligible.

Differential scanning calorimetry (DSC) measurements employed a Du Pont Model 900 thermal analyzer. Sample size was standardized at 20.2 mg. The heating rate was 10°/min. The instrument was calibrated with fusion endotherms of mercury, gallium, and indium.

The laser-light-scattering experiment utilized a Spectra-Physics Model 132 helium-neon gas laser.

Results

Wide-Angle X-Ray Data. General. Wide-angle X-ray scattering data were obtained for salts of ethylene-methacrylic acid and butadiene-methacrylic acid copolymers, poly(methacrylic acid), methacrylic acid, and acetic acid. Except where indicated in the following figures direct comparison of scattering intensities is possible.

Figure 1 shows the effect of ionization on the "ionomer peak" of a dry B-MAA copolymer containing 10.5 wt % MAA. The scattering intensity increases as the amount of metal ion incorporated increases. A definite peak is observed at higher levels of ionization.

Figure 2 shows the effect of acid content in the copolymer for completely ionized dry B-MAA copolymers containing 7, 10.5, and 18 wt % MAA. The scattering intensi-

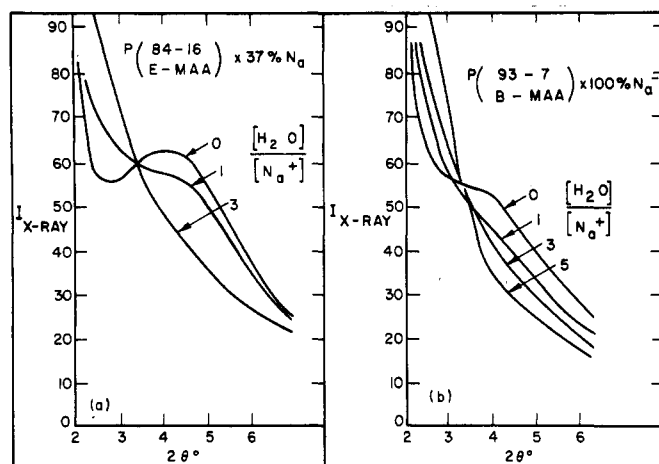


Figure 4. Effect of non-equilibrium water absorption on the X-ray peak of ionomers. (a) 84-16 wt % E-MAA copolymer ionized 37% with sodium; (b) 93-7 wt % B-MAA copolymer ionized 100% with sodium.

ty increases as the amount of metal ion incorporated increases. The peak also moves to higher angles, indicating a smaller Bragg spacing, as the MAA content is increased.

The X-ray scattering of poly(methacrylic acid) (PMAA) and its dry, partially ionized salt was recorded. As observed by Wilson, Longworth, and Vaughan,⁸ a peak appears in the polyelectrolyte at $2\theta = 7.5^\circ$ which corresponds to a Bragg spacing of 11.8 Å.

The approximately 20-Å ionomer peak, of the polyethylene ionomers studied appeared at angles comparable to values reported by Wilson, Longworth, and Vaughn.⁸ The data are presented in the Discussion section.

The sodium salts of acetic acid (HOAc) and methacrylic acid (MAA) were studied. These were prepared by adding sodium hydroxide powder to the respective acids. It was observed that for ionization levels of the acids of less than one-third, two phases were formed, a partially ionized white phase and a less dense unionized clear phase. At one-third ionization a homogeneous material with a waxy consistency resulted. At higher degrees of ionization crystallites were visually evident and the X-ray diffraction became very crystalline.

X-Ray scattering scans were obtained for samples of acetic and methacrylic acid samples ionized one-third. Peaks, which are not present in X-ray scattering from the unionized acids, occur at angles of 2θ equal to 11.1 and 9.2° for the HOAc and MAA salts, corresponding to Bragg spacings of 8.0 and 9.6 Å. Examination of the X-ray scattering of the more dense phase of the molecular acids ionized less than one-third indicated the same angle of scattering for partially ionized MAA, but an angle closer to 10.5° corresponding to a Bragg spacing of 8.4 Å for partially ionized HOAc.

Effect of Elevated Temperature. Figure 3 shows the effect of temperature on the polyethylene ionomer X-ray peak. As the temperature is raised, the X-ray peak persists and shifts to lower angles indicating a larger spacing. The "ionomer" peak persists to well above the melting point of the polyethylene portion of the copolymer.

Non-Equilibrium Absorption Experiments. Two types of experiments were undertaken to study the effect of polar plasticizers on the ionomer X-ray peak. Non-equilibrium absorption experiments are described in this section. Plasticizers were distributed unevenly in the samples in a manner determined by the rate of diffusion of plasticizer into the sample. Sample geometries were approximately the same in all cases.

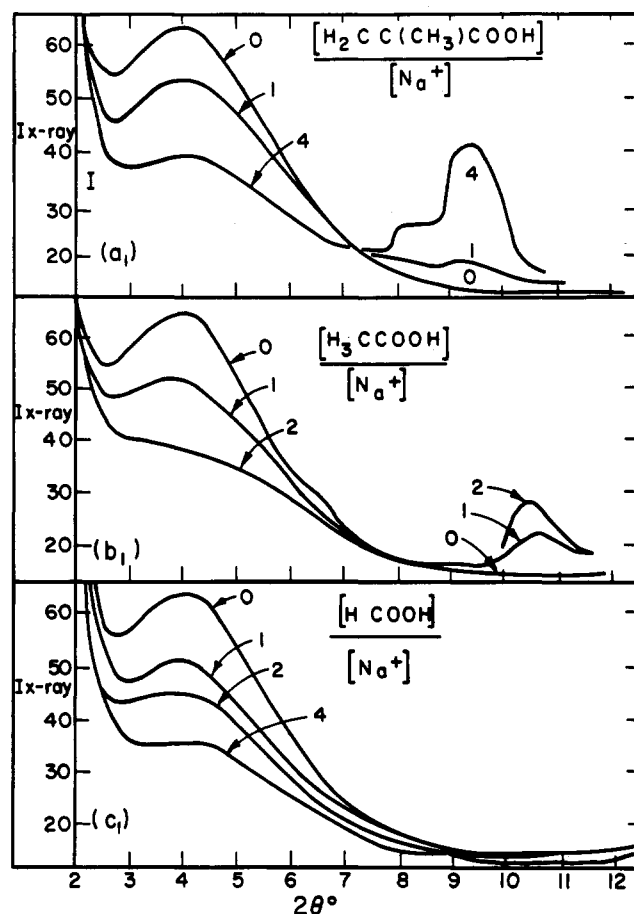


Figure 5. Effect of non-equilibrium acid absorption on the ionomer X-ray peak of an 84-16 wt % E-MAA copolymer ionized 37% with sodium: (a) absorption of methacrylic acid; (b) absorption of acetic acid; (c) absorption of formic acid.

Figure 4 shows the effect of water absorption on the ionomer X-ray peak of an E-MAA ionomer and of a B-MAA ionomer. The number of water molecules added per metal ion in the ionomer is indicated in the figure. The effect of water on both materials is qualitatively the same. In both cases the scattering intensity decreases at large angles and increases at small angles.

The effect of methanol absorption on the ionomer X-ray peak of an E-MAA ionomer and of a B-MAA ionomer was studied. In both systems the scattering intensity decreased at all angles.

Figure 5 shows the effect of methacrylic acid, acetic acid, and formic acid on the ionomer peak of an E-MAA ionomer. The effect of these acids on a B-MAA ionomer was similar. It can be seen that the X-ray peak characteristic of the polymers decreases and is replaced by peaks characteristic of the partially ionized molecular acids.

Equilibrium Absorption Experiments. The butadiene ionomer studied in the preceding section was 100% ionized. As a result of this high degree of ionization and the lack of crystallinity in this system, water absorption was much faster than for the ethylene ionomer studied. Thus it required only a few hours to acquire the data in Figure 4b for the butadiene ionomer but to acquire the data in figure 4a for the ethylene ionomer required months. For this reason butadiene ionomers were selected for equilibrium absorption experiments.

Butadiene ionomer samples were exposed to the vapor of the polar plasticizer until a desired amount of plasticizer had been absorbed. Samples were then sealed in glass jars for two or more days to achieve homogeneous plasti-

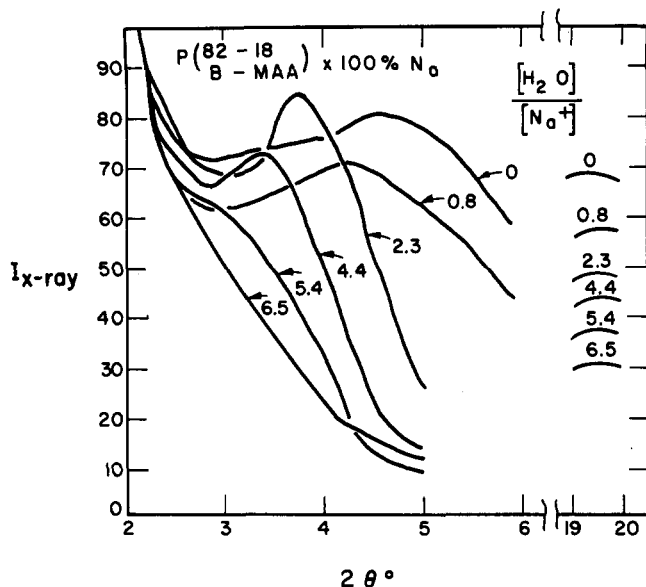


Figure 6. Effect of equilibrium water absorption on the ionomer X-ray peak of an 82-18 wt % B-MAA copolymer ionized 100% with sodium.

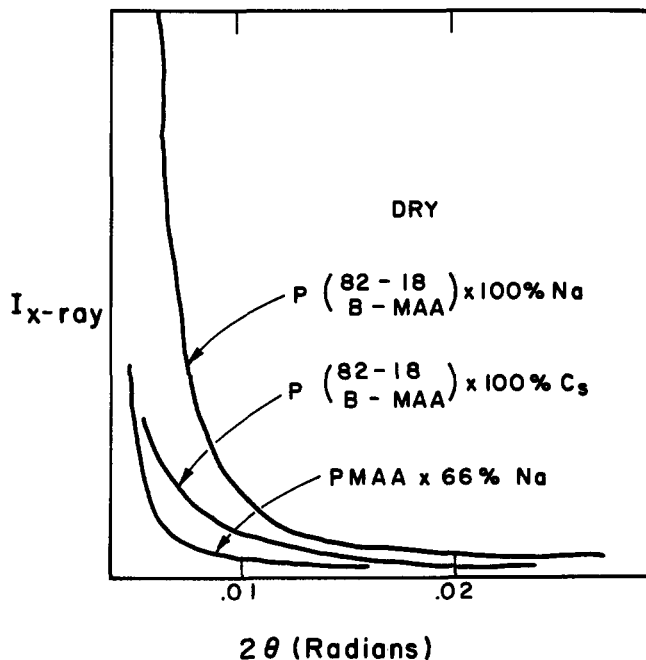


Figure 7. Small-angle X-ray scattering for dry butadiene and methacrylic acid ionomers.

cizer distribution. The weight of the dry samples with no plasticizer absorbed was determined by drying in a vacuum oven at 80° to constant weight.

The effect of methanol was to decrease the intensity of both the ionomer peak and the amorphous hydrocarbon X-ray peak (at $2\theta \approx 19^\circ$).

Figure 6 presents the effect of water on the ionomer peak and the amorphous hydrocarbon X-ray peak of a completely ionized B-MAA copolymer containing 18 wt % MAA. Similar results were obtained for an ionized B-MAA copolymer containing 10.5 wt % MAA. For both ionomers the "ionomer peak" shifts to lower angles corresponding to larger Bragg spacings as water is added.

The data in Figure 6 correspond to equilibrium values. Storing the sample longer than 2 days did not affect the peak location and the same peak location was obtained either by addition of water to a dry sample or removal of water from a wet sample.

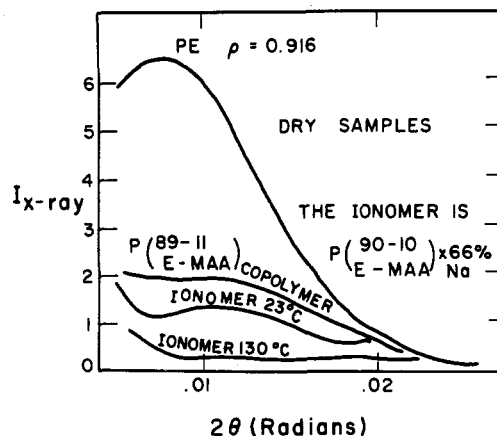


Figure 8. Small-angle X-ray scattering of a low-density polyethylene, an E-MAA copolymer, an E-MAA ionomer, and a molten E-MAA ionomer.

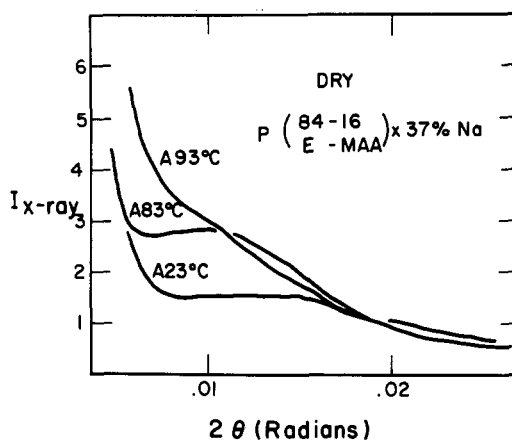


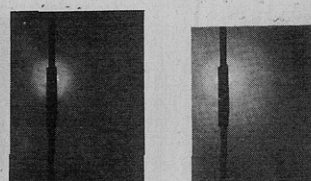
Figure 9. Small-angle X-ray scattering for an E-MAA ionomer as a function of annealing temperature.

Small-Angle X-Ray Data. Figure 7 represents data of small-angle X-ray scattering (SAXS) intensity as a function of angle for the dry sodium and cesium salts of a butadiene-methacrylic acid ionomer and for the dry sodium salt of poly(methacrylic acid). None of these materials exhibit a small-angle X-ray scattering peak. The relative intensities of X-ray scattering in Figure 7 are not directly comparable since it was necessary to use different sample thicknesses for each material.

Figure 8 shows the effect of copolymerization and ionization of the (SAXS) of an ethylene-methacrylic acid ionomer. The figure presents small-angle X-ray scattering data for dry samples of a low-density polyethylene, an E-MAA copolymer, an E-MAA sodium ionomer, and the same ionomer at 130°. The intensity of small-angle X-ray scattering is reduced by copolymerization and ionization. The small-angle X-ray scattering is absent in the molten ionomer.

Figure 9 shows the effect of annealing on the small-angle X-ray scattering of a dry ethylene-methacrylic acid ionomer. Annealing at successively higher temperatures causes the intensity of scattering and the average Bragg spacing to increase.

Figure 10 presents photographs of the small-angle X-ray scattering of a dry and partially wet E-MAA ionomer. The wet sample contained about 5 wt % water and was the same sample used to obtain the wide-angle X-ray data in Figure 4a. In addition to the scattering ring of the dry ionomer, the wet ionomer exhibits a second ring at larger angles. It is suggested in the discussion that the second



a) DRY b) WET

Figure 10. Effect of water on the small-angle X-ray scattering of an 84-16 wt % E-MAA copolymer ionized 37% with sodium.

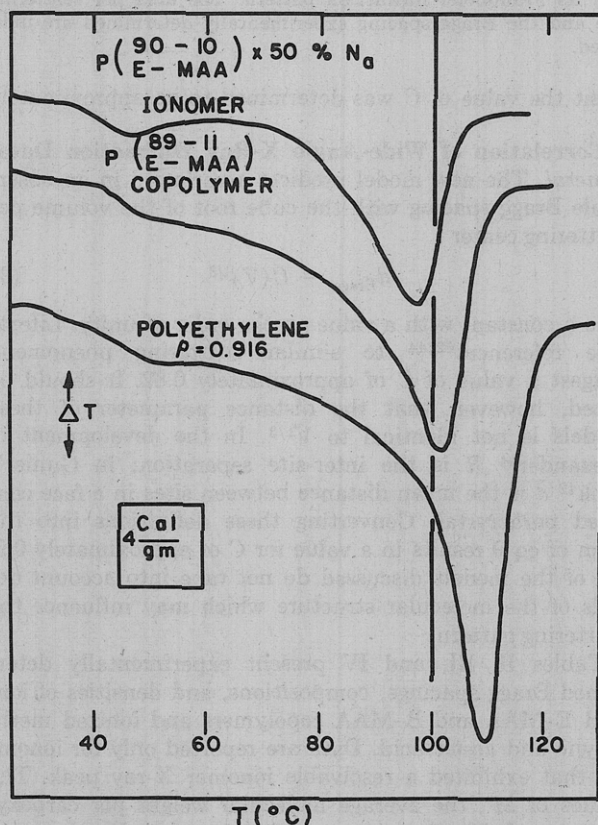


Figure 11. DSC results showing the effect of copolymerization and ionization on the crystallinity and melting point of E-MAA ionomers.

ring is the wide-angle X-ray "ionomer peak" that has moved into the small-angle X-ray scattering region.

DSC Data. Figure 11 presents DSC curves which show the effect of copolymerization and ionization on the melting behavior of an ethylene-methacrylic acid ionomer. The figure presents DSC curves for a low-density polyethylene, an E-MAA copolymer, and an E-MAA sodium ionomer. A scale marker on the figure indicates the amount of area that corresponds to a crystalline melting endotherm of 4 cal/g. The amount of crystallinity and the melting point are reduced by copolymerization and ionization.

Figure 12 shows the effect of annealing on the DSC curves of a dry E-MAA ionomer. Annealing at successively higher temperatures causes the highest melting point to increase.

Discussion

New Morphological Model. A new ionomer morphological model is proposed. The new "aggregate" model consists of acid aggregates homogeneously distributed in the amorphous phase. The aggregates contain two or more carboxyl groups depending on the composition of the co-

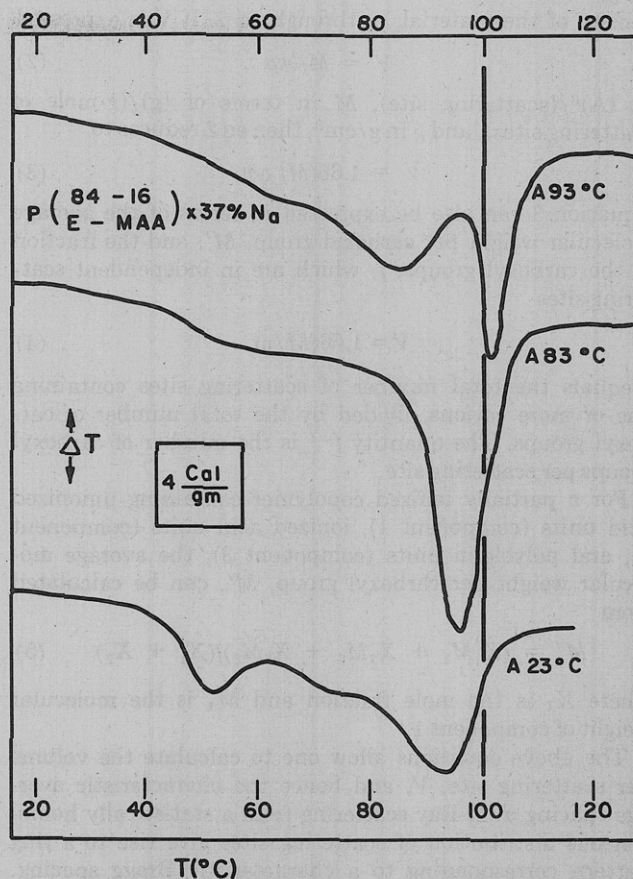


Figure 12. DSC results showing the effect of annealing on the crystallinity and melting points of the E-MAA ionomer investigated by small-angle X-ray scattering.

polymer and the amount of water present. The aggregates contain both protons and metal ions. The aggregates are thought to have a linear dimension on the order of 5-10 Å and hence a volume on the order of 10^3 Å^3 . The aggregates are therefore orders of magnitude smaller than the ionic clusters theorized in the "cluster" model which have a linear dimension of approximately 100 Å and hence a volume of approximately 10^6 Å^3 .

X-Ray Scattering Analysis. In this section an analysis of ionomer X-ray scattering is presented which assumes that an electron density difference exists in ionomers which results from the presence of cations. This assumption is different from that made for the cluster model which assumes that the electron density difference present in ionomers but not in the unionized copolymers results from a change in aggregation. In the new model, X-ray scattering is assumed to be similar to the scattering of liquids. It is assumed that the scattering results from scattering sites containing one or more cations which are homogeneously distributed throughout the amorphous phase of the polymer. These scattering sites are analyzed as point scatterers.

For a homogeneous distribution of scattering points one can define a characteristic distance, d , between scattering points. This distance is simply related to the two-dimensional average area per scattering point, A , and to the three-dimensional average volume per scattering point, V

$$d = (A)^{1/2} = (V)^{1/3} \quad (1)$$

V is the total volume of material divided by the total number of scattering points in that volume. V is related to the average molecular weight associated with each scattering point, M , Avogadro's number, N , and the average

density of the material, ρ , through eq 2. If V is expressed

$$V = M/N\rho \quad (2)$$

in $(\text{\AA})^3/(\text{scattering site})$, M in terms of $(\text{g})/(\text{g-mole of scattering sites})$, and ρ in g/cm^3 , then eq 2 reduces to

$$V = 1.66(M/\rho) \quad (3)$$

Equation 3 can also be expressed in terms of the average molecular weight per carboxyl group, M' , and the fraction of the carboxyl groups, f , which are in independent scattering sites

$$V = 1.66(M/\rho) \quad (4)$$

f equals the total number of scattering sites containing one or more cations divided by the total number of carboxyl groups. The quantity f^{-1} is the number of carboxyl groups per scattering site.

For a partially ionized copolymer containing unionized acid units (component 1), ionized acid units (component 2), and polyolefin units (component 3), the average molecular weight per carboxyl group, M' , can be calculated from

$$M' = (X_1M_1 + X_2M_2 + X_3M_3)/(X_1 + X_2) \quad (5)$$

where X_1 is the mole fraction and M_1 is the molecular weight of component 1.

The above equations allow one to calculate the volume per scattering site, V , and hence the characteristic average spacing d . X-Ray scattering from a statistically homogeneous distribution of scattering sites give rise to a ring pattern corresponding to a characteristic Bragg spacing. The Bragg spacing, d_{Bragg} , is simply related to the spacing d by

$$d_{\text{Bragg}} = Cd \quad (6)$$

where C is a constant on the order of unity.⁴²

Once the constant C is determined, experimentally determined Bragg spacings can be correlated with the calculated volume per carboxyl group, V' , using

$$d_{\text{Bragg}} = C(V'f^{-1})^{1/3} \quad (7)$$

From this correlation the value of f^{-1} , the number of carboxyl groups per scattering site, can be determined.

Light Scattering Analog. An attempt was made to experimentally determine the value of the constant C in eq 6. The physics of light scattering is the same as the physics of X-ray scattering. Since the wavelength of light is about 2000 times the wavelength of X-rays, a pictorial model 2000 times larger than the structure giving rise to X-ray scattering will produce an identical light scattering image.

Figure 13a is a statistically homogeneous lattice of scattering sites.⁴³ This pattern is similar to the pattern of scattering sites assumed to be present in ionomers. Figure 13a was photographically reduced in size on a negative and the negative placed in a beam of laser light. Figure 13b is the Fraunhofer diffraction pattern produced. The area per scattering site, A , was measured in Figure 13a and the Bragg spacing (eq 8) was computed. Inserting

$$d_{\text{Bragg}} = \frac{\lambda}{(2 \sin \theta) \text{ maximum intensity}} \quad (8)$$

these values of d_{Bragg} and A for the negative into eq 6 and 1 allowed calculation of the constant C . By this experi-

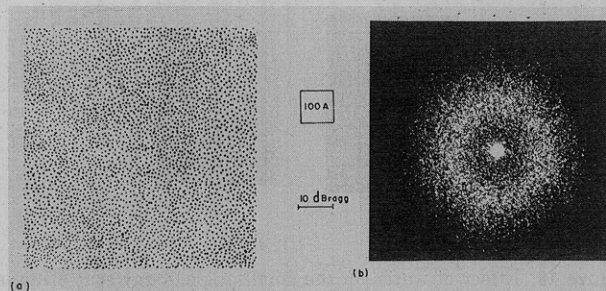


Figure 13. A statistically homogeneous lattice of scattering sites and its Fraunhofer diffraction pattern. The area per scattering site and the Bragg spacing experimentally determined are indicated.

ment the value of C was determined to be approximately 1.1.

Correlation of Wide-Angle X-Ray Diffraction Data.

General. The new model predicts a variation in an observable Bragg spacing with the cube root of the volume per scattering center

$$d_{\text{Bragg}} = C(V)^{1/3} \quad (9)$$

C is a constant with a value on the order of unity. Literature references^{42,44} to similar scattering phenomena suggest a value of C of approximately 0.82. It should be noted, however, that the distance parameter of these models is not identical to $V^{1/3}$. In the development of Alexander⁴⁴ R is the inter-site separation; in Guinier's book⁴² \bar{d} is the mean distance between sites in a face centered paracrystal. Converting these definitions into the form of eq 9 results in a value for C of approximately 0.9. All of the models discussed do not take into account details of the molecular structure which may influence the scattering pattern.

Tables II, III, and IV present experimentally determined Bragg spacings, compositions, and densities of ionized E-MAA and B-MAA copolymers and ionized methacrylic and acetic acid. Data are reported only for ionomers that exhibited a resolvable ionomer X-ray peak. The values of M' , the average molecular weight per carboxyl group, and V' , the average volume per carboxyl group, calculated from the composition and density are also presented. Values of V in the tables were computed with the values of f^{-1} , the number of carboxyl groups per scattering center, indicated in the table. Integer values of f^{-1} were chosen which resulted in the best fit of a line with a slope of $1/3$ on a log-log plot of Bragg spacing as a function of volume per scattering site. The line chosen was constrained by the consideration that it should be a reasonably good fit of the data for partially ionized MAA and HOAc. The behavior exhibited by partially ionized MAA and HOAc indicates that carboxyl groups in these partially ionized molecular acids aggregate as trimers. By this interpretation, at one-third ionized each trimer aggregate contains one sodium ion. Below one-third ionized the phase separation indicates that some of the acid is not associated with metal ions and forms an unionized clear phase. Therefore it is concluded that for these molecular acids the acid groups aggregate as trimers and f^{-1} equals 3. Inserting the values of f , V' , and d_{Bragg} for these monomeric acids into eq 7 indicates that the value of the constant C is between 1.2 and 1.3.

Points corresponding to the experimentally determined Bragg spacings and the calculated volume per scattering center giving rise to the ionomer peak are presented in

(42) A Guinier and G. Fournet, "Small-Angle Scattering of X-rays," Wiley, New York, N. Y., 1955, p 143.

(43) R. Hosemann and S. W. Bagchi, "Direct Analyses of Diffraction by Matter," North Holland Publishing Co., Amsterdam, 1962, p 563.

(44) L. E. Alexander, "X-ray Diffraction Methods in Polymer Science," Wiley Interscience, New York, N. Y., 1969, p 381.

Table II
Volume per Scattering Site Calculations for E-MAA Ionomers

% MAA		Ionized		Ref	$M' \times 10^{-2}$	ρ^b	$V' \times 10^{-2}$	f^{-1d}	$V \times 10^{-2}$	d_{Bragg}^f
Wt	Mol	Ion	%							
5	1.7	Na ^g	90	WLV ^h	17.3	0.92 ^j	31.3	2	62.4	24
8	2.8	Na ^g	63	WLV	10.7	0.94 ^j	19.1	2.5	47.6	22
8	2.8	Na ^g	90	WLV	10.8	0.93 ^j	19.4	2.5	48.2	27
10	3.6	Na	50	M&C ⁱ	8.5	0.941	15.0	3	44.8	22
10	3.6	Na	75	M&C	8.5	0.940	15.1	3	45.2	23
11	3.9	Na ^g	45	WLV	8.0	0.94 ^j	14.2	3	42.4	21
11	3.9	Na ^g	68	WLV	8.0	0.94 ^j	14.2	3	42.4	23
12	4.3	Zn	57	M&C	7.3	0.960	12.7	3	37.8	21
15	5.3	Na	29	M&C	5.9	0.950	10.4	3	31.0	19
16	6.0	Na	37	M&C	5.3	0.957	9.3	4	37.0	21
17	6.25	Na ^g	28	WLV	5.1	0.95 ^j	9.0	4	35.6	19
17	6.25	Na ^g	43	WLV	5.2	0.96 ^j	9.0	4	35.8	20
100	100	Na	66	M&C	1.01	1.53	1.09	7	7.6	11.7

^a M' is the calculated average molecular weight per acid group (g/g mol). ^b ρ is the average density (g/cm³). ^c V' is the calculated average volume per carboxyl group (Å³). ^d f^{-1} is the assumed number of acid groups per scattering site. ^e V is the calculated volume per scattering site (Å³). ^f d_{Bragg} is the experimentally determined Bragg spacing (Å). ^g Assumed. ^h Wilson, Longworth, and Vaughan.⁸ ⁱ Marx and Cooper (this work). ^j Estimated from $\phi_{\text{E,cryst}}$ correlation.¹⁴

Table III
Volume per Scattering Site Calculations for B-MAA Ionomers

MAA Content		Ionized		M'	ρ	$V' \times 10^{-2}$	f^{-1}	$V \times 10^{-2}$	d_{Bragg}
Wt %	Mol %	Ion	%						
7.0	4.6	Na	100	12.3	0.938	21.7	3	65.2	25
10.5	6.9	Na	66	8.3	0.946	14.5	3	43.6	21.5
10.5	6.9	Na	100	8.4	0.956	14.5	3	43.6	21.5
18.0	12.0	Na	100	5.0	1.00	8.4	4	33.5	19
100	100	Na	66	1.01	1.53	1.09	7	7.6	11.8

Table IV
Volume per Scattering Site Calculations for Partially Ionized Molecular Acids

Acid	ρ	M'	$V \times 10^{-2}$	f^{-1}	$V \times 10^{-2}$	d_{Bragg}
MAA·½NaOH	1.15	97.3	1.40	3	4.21	9.6
HOAC·½NaOH	1.23	73.3	0.99	3	2.97	8.0, 8.4

Figure 14. It can be seen that

$$d_{\text{Bragg}} = 1.3(V)^{1/3} \quad (10)$$

is a good fit of the data. The value of 1.3 for the constant is slightly higher than the value of 1.1 determined by the light scattering analog and 0.9 reported in the literature. One data point from data of Longworth, and Vaughan noticeably does not fit the correlation. In the following section it is shown that the large Bragg spacing for this data point probably resulted because their sample was wet.

Most of the polyethylene ionomers studied are about 30% crystalline.⁸ Since the salt groups are excluded from the crystalline phase^{5,34,35} the concentration of these groups in the amorphous phase is greater than the total average concentration. Therefore plotting $V(\text{amorphous phase})$ rather than $V(\text{total})$ in Figure 14 would shift the polyethylene ionomer data points to 30% lower values of V for the same values of f^{-1} or require 30% higher values of f^{-1} to obtain the values of V in Figure 14.

Table V presents values of f^{-1} , determined by obtaining the best fit of the data in Figure 14. It is observed that as the acid concentration increases, the degree of association increases from dimers to trimers to tetramers, up to septimers. These aggregates are much smaller than the 100-Å diameter domain envisioned in the cluster model.

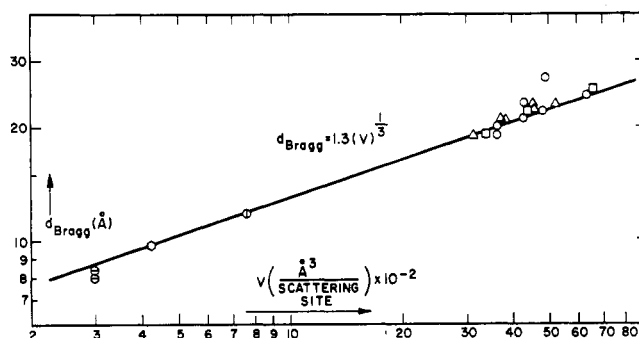


Figure 14. Plot of Bragg spacing as a function of volume per scattering site. Data for P(E-MAA) ionomers: (Δ) this work; (\circ) Wilson, Longworth, and Vaughan.⁸ Data for P(B-MAA) ionomers: (\square) this work. Data for P(MAA) ionomer: (\oplus) this work. Data for MAA·½NaOH: (\circ) this work. Data for HAC·½NaOH: (\ominus) this work.

The increasing acid group concentration results in a shorter average segment length between acid groups. This appears to increase the possibility of acid group interaction which allows the formation of larger aggregates. It is of interest that for ionized poly(methacrylic acid) the aggregation is approximately 7, which is very close to the value deduced by Eisenberg¹⁸ from steric arguments.

From Table V it can be seen that the transitions from dimers to trimers and from trimers to tetramers occur at about 5 and 11 vol % MAA in the copolymer.

Five volume per cent MAA in a styrene copolymer corresponds to about 7 mol % MAA. Eisenberg and Navratil^{16,17,45} reported a transition at about 7 mol % MAA which they interpreted as a clustering transition.

(45) A. Eisenberg and M. Navratil, Personal Communication.

Table V
Acid Association as a Function of Composition^a

Copolymer Composition (% MAA)		Comonomer Ethylene and Butadiene	f^{-1}	Carboxyl Group Aggregation
Vol %	Wt %			
4	5	E	2	Dimers
6	8	E	2.5	
6	7	B	3	Trimers
7	10	E	3	Trimers
8	11	E	3	Trimers
9	11	B	3	Trimers
9	12	E	3	Trimers
10	14.5	E	3	Trimers
12	16	E	4	Tetramers
12	17	E	4	Tetramers
15	18	B	4	Tetramers
100	100		7	Septimers

^a f^{-1} is the assumed number of carboxyl groups per scattering site.

Below 5.5 mol % MAA the S-MAA ionomers obey time temperature superposition and the ionomers absorb only one water molecule per metal ion. Above 7.9 mol % MAA, time-temperature superposition is inapplicable, water absorption is greater than one water molecule per metal ion, and a low-angle X-ray peak is observed for cesium salts. This work suggests that the transition observed by Eisenberg and Navratil corresponds to the transition from dimer to trimer aggregates.

Effect of Elevated Temperatures. The new model qualitatively explains the presence of the polyethylene ionomer X-ray peak at high temperatures, and predicts a shift in the peak to lower angles indicating a larger spacing between scattering centers. This shift is predicted since the elevated temperature reduces the degree of ethylene crystallinity and causes thermal expansion. Both of these changes result in a greater separation of scattering sites. A change in the peak location would also result from a change in the number of acid groups per scattering site. Figure 3 indicates that the peak persists at higher temperatures and shifts to smaller angles corresponding to larger Bragg spacings.

Absorption Experiments. It was shown above that molecular acids and methanol cause the ionomer peak to diminish while water shifts it to smaller angles. Acetic and methacrylic acid also cause a new ionomer peak at an angle corresponding to the pure ionized molecular acid.

The effect of molecular acids on the X-ray ionomer peak is to be expected since the low molecular weight acids have larger dissociation constants than polymerized methacrylic acid.⁴⁶ Therefore the metal ions are extracted from the ionomer by the acid diluent.

Methanol is a molecule with a hydroxyl group on one end which is compatible with the ionic scattering sites. The methyl group on the other end is compatible with the surrounding hydrocarbon matrix. Therefore the methanol molecules would be expected to encircle the scattering sites. The decrease in the detectability of the ionomer peak apparently results because addition of methanol to the scattering sites decreases the electron density difference in the system.

Water is a molecule which is completely compatible with the ionic sites. It has been shown that the volume per scattering site is proportional to the cube of the exper-

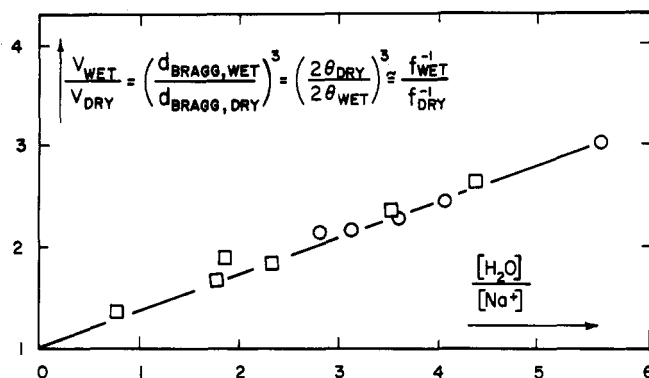


Figure 15. Equilibrium ionic aggregate size as a function of water content.

Symbol	Wt % Composition	Dry	
		$2\theta^\circ$	$d_{\text{Bragg}} (\text{\AA})$
□	$P^{(82-18)}_{\text{B-MAA}} \times 100\% \text{ Na}$	4.65	19
○	$P^{(89.5-10.5)}_{\text{B-MAA}} \times 100\% \text{ Na}$	4.1	21.5

imentally measured Bragg spacing. From eq 4 it can be seen that the volume per scattering site is a function of the molecular weight per acid group, M' , the average ionomer density, ρ , and the number of acid groups per scattering site, f^{-1} . The large change in the observed Bragg spacing cannot be accounted for by the small changes in M' and ρ that result from water addition. Hence the observed change in the Bragg spacing must result from a change in the number of acid groups per scattering site.

In light of the preceding discussion it seems reasonable that as the ratio of water molecules to metal ions, $[\text{H}_2\text{O}]:[\text{Na}^+]$, increases, the average number of acid groups in each cluster, f^{-1} , which is proportional to $(d_{\text{Bragg}})^3$, will also increase. Figure 15 is a plot of these two quantities as a function of each other. This plot was prepared using data of scattering angle maximum as a function of ionomer water content. Data on the 18 wt % MAA butadiene ionomer ionized 100% was presented in Figure 6. For both ionomers the average number of acid groups in each aggregate increases in a linear fashion as the number of water molecules per metal ion increases.

Small-Angle X-Ray and DSC Data. The major conclusion to be drawn from Figures 7, 8, and 9 is that the small-angle X-ray scattering peak in dry polyethylene ionomers is caused by polyethylene crystalline lamellar spacings, not by ionic clusters.

From the DSC data (Figures 11 and 12) and the small-angle X-ray data (Figures 8 and 9), it can be observed that the melting point and the Bragg spacing are closely related. Similarly the amount of crystallinity in the DSC endotherms of Figure 11 and the intensity of small-angle X-ray scattering in Figure 8 are related. The small-angle X-ray scattering is absent above the melting point of the ethylene ionomer and is also absent for noncrystalline ionomers. These results indicate that the small-angle X-ray scattering is caused by polyethylene crystalline lamellae.

Figures 4 and 6 presented wide-angle X-ray data showing the effect of addition of water to ionomers. The data revealed a shift of the "ionomer X-ray peak" to smaller and smaller angles, until it moved to a sufficiently small angle that it can no longer be detected in the wide-angle X-ray scattering region.

Figure 10 presented small-angle X-ray photographs of a dry and partially wet E-MAA ionomer. These figures

(46) M. L. Miller, "The Structure of Polymers," Reinhold, New York, N. Y., 1966, p 589.

suggest that water absorption shifts the "20-Å wide-angle ionomer peak" into the small-angle X-ray region.

Delf and MacKnight¹⁵ reported a small-angle X-ray scattering peak at an angle of 0.018 rad for ethylene-methacrylic acid ionomers ionized 60% with sodium and cesium but reported no peak for the lithium ionomer. The new data presented in this work would suggest that the low-angle peak they reported was caused by an overlap of the polyethylene crystalline lamellar peak and the "wide-angle X-ray ionomer peak" that shifted to smaller angles as a result of moisture absorption.

Conclusions⁴⁷

This work introduces a new "aggregate" model for the morphology of ionomers. The model consists of small acid aggregates homogeneously distributed throughout the amorphous phase. The new model successfully correlates

the physical properties and morphology of ionomer systems. As a result of this study several new conclusions can be drawn about the structure of ionomers. (1) The wide-angle "ionomer X-ray peak" Bragg spacing is a measure of the average distance between ionic scattering sites. (2) The degree of acid group aggregation in dry ionomers increases from dimers to trimers to tetramers up to septimers as the acid content in the copolymer increases. (3) Plasticization with water increases the extent of acid group aggregation. (4) Low-angle X-ray scattering results from crystalline lamellae in ethylene ionomers and from the "ionomer X-ray peak" shifted to lower angles as a result of water plasticization.

Acknowledgments. The authors thank Dr. E. A. Collins and Mr. D. G. Fraser of the B. F. Goodrich Chemical Co. and Mr. W. F. Brondyke of the E. I. du Pont de Nemours & Co. for supplying the butadiene copolymers and ethylene ionomers used in this study. We thank Mr. R. A. Horn of the Forest Products Laboratory for making the LAXS densitometer measurements. Finally we are grateful for partial federal support of this research through the National Science Foundation and the National Defense Education Act.

(47) **Note Added in Proof.** In a recent note, F. L. Binsbergen and G. F. Kroon (*Macromolecules*, **6**, 145 (1973)) have presented an explanation of the ionomer X-ray peak. Their interpretation, that the ionomer peak arises from constructive interference due to a most frequently occurring distance between nearest-neighbor clusters, is essentially identical with the "aggregate model" proposal of this paper.

Homopolymer and Random Copolymer Solubility in Styrene- α -Methylstyrene Systems

D. J. Goldwasser and D. J. Williams*

Department of Chemical Engineering, The City College of The City University of New York, New York, New York 10031. Received February 28, 1973

ABSTRACT: We report on an experimental study of the solution properties of well-tailored homopolymers and copolymers of styrene and α -methylstyrene, prepared *via* the living polymer technique. In accord with earlier investigations, we found evidence of an increased copolymer solubility over that obtained by linear interpolation between the parent homopolymers. This effect is most pronounced in plots of Θ temperatures *vs.* composition which show minima. This phenomenon is also shown to be manifested in Flory-Huggins parameters obtained for moderately concentrated (3–25 vol %) toluene solutions. Comparison of our results with those available in the literature reinforce the notion that such increases in copolymer solubility are quite general, if not universal. The interactions accounting for the enhanced solubility were correlated in terms of an interunit interaction parameter

χ_{ab} .

A major obstacle to a fundamental understanding of the processes controlling polymer solution thermodynamics is our lack of empirical knowledge of the molecular factors controlling the equilibrium state. For example, one would like to relate such molecular factors as functional group composition, repeat unit structure, copolymer composition, and tacticity to actual polymer solution behavior. This goal requires extensive thermodynamic data on model polymer solutions. In the current research we have studied the solution properties of a series of well-tailored homopolymers and random copolymers constructed from the closely related monomers styrene and α -methylstyrene. Differences in the solution properties of the materials of interest would pertain specifically to the number and location of the methyl group. The polymers were synthesized by the anionic living-polymer reaction to produce amorphous materials with fairly narrow molecular weight distributions. In addition the copolymers were homogeneous and random, and had compositions of 24, 50, and 69 wt % styrene.

Several groups of researchers have studied the thermodynamic and conformational properties of random copoly-

mers in dilute solution.^{1–6} The materials receiving the most attention are based on styrene and the various esters of acrylic and methacrylic acid. A salient finding to emerge from these studies is an increase in copolymer solubility over that exhibited by the parent homopolymers. The evidence for this enhanced solubility is summarized in Table I. The parameters directly and unambiguously measured are the second virial coefficient (A_2), the theta temperature (Θ), and the intrinsic viscosity ($[\eta]$), whereas the long-range interaction parameter (B) must be derived from still-imperfect two-parameter theories.⁷ The param-

- (1) W. H. Stockmayer, L. D. Moore, Jr., M. Fixman, and B. N. Epstein, *J. Polym. Sci.*, **14**, 517 (1955).
- (2) A. Kotera, T. Saito, Y. Watanabe, and M. Ohama, *Makromol. Chem.*, **87**, 195 (1965).
- (3) Y. Shimura, *J. Polym. Sci., Part A-2*, **4**, 423 (1966).
- (4) T. Kotaka, Y. Murakami, and H. Inagaki, *J. Phys. Chem.*, **72**, 869 (1968).
- (5) H. Matsuda, K. Yamano, and H. Inagaki, *J. Polym. Sci., Part A-2*, **7**, 609 (1969).
- (6) W. Mächtle, *Angew. Makromol. Chem.*, **10**, 1 (1970).
- (7) H. Yamakawa, "Modern Theory of Polymer Solutions," Harper & Row, New York, N. Y., 1971.